13th International Conference on
Structural Health Monitoring of Intelligent Infrastructure
DOI: 10.3217/978-3-99161-057-1-029

DFOS-Based Monitoring of Prestressed Concrete Bridge Girders

Kleo Lila[1], Max Herbers[1], Bertram Richter[1], Andrea Agreiter[2], Maja Kreslin[3], Petra Triller[3], Andrej Anžlin[3], Werner Lienhart[2], Steffen Marx[1]
[1]Institute of Concrete Structures, TUD Dresden University of Technology,
01062 Dresden, Germany
[2]Institute of Engineering Geodesy and Measurement Systems, Faculty of Mathematics, Physics and Geodesy, Graz University of Technology, Steyrergasse 30, 8010 Graz, Austria
[3] Slovenian National Building and Civil Engineering Institute, Dimičeva ulica 12, SI 1000 Ljubljana, Slovenia
email: @ kleo.lila@tu-dresden.de, @ max.herbers@tu-dresden.de, @ bertram.richter@tu-dresden.de @ andrea.agreiter@tugraz.at, @ andrej.anzlin@zag.si, @ maja.kreslin@zag.si, @ petra.triller@zag.si @ werner.lienhart@tugraz.at @ steffen.marx1@tu-dresden.de

ABSTRACT: Due to bridges' critical role in transportation networks, the assessment and maintenance of existing bridges have become a priority. Prestressed concrete bridges constitute a significant portion of Europe's transportation network, yet many no longer meet today's technical requirements. This is primarily due to two factors: (i) the unforeseen increase in heavy goods traffic, and (ii) insufficient experience with early reinforced and prestressed concrete construction methods, coupled with inadequate regulations, which resulted in design weaknesses and structural deficiencies. One critical failure mechanism, identified when recalculating existing bridges based on updated guidelines, is insufficient shear load-bearing capacity, which has prompted the premature demolition of numerous bridges. A thorough understanding and rigorous monitoring of shear behavior is essential since neglecting this problem could lead to notable consequences, especially for aging infrastructure. In this paper, a distributed fiber optic sensor (DFOS) based monitoring system, inspired by shear detection concepts, is tested. A decommissioned prestressed concrete bridge girder was equipped with a DFOS grid, allowing for detailed monitoring of crack width, location, and shape. Preliminary test results confirm the successful installation and early detection of cracks, highlighting the system's potential to identify microcrack formation, monitor crack growth, and support maintenance strategies.

KEYWORDS: Structural Health Monitoring; Distributed Fiber Optic Sensors; Microcracking; Crack Growths; Load Testing; Prestressed Concrete.

1 INTRODUCTION

Concrete serves as the cornerstone of contemporary infrastructure, valued for its adaptability, strength and longevity. Nonetheless, despite its formidable exterior, concrete exhibits inherent material characteristics that, if neglected, may result in structural failures. Among these, shear forces are a critical and complex failure mechanism, due to the brittle behavior. Improper management of shear stresses may lead to abrupt, severe cracking, endangering the service life and safety of infrastructures such as bridges. One of the reasons for this is that these aging bridges were originally designed for lower traffic loads, and this issue is intensified by the absence or insufficient shear reinforcement [1], [2]. Modern codes surpass traditional visual inspections in terms of objectivity, repeatability, and sensitivity, imposing higher safety margins, often revealing structural deficiencies when existing bridges are recalculated for shear strength.

Unlike flexural failures, which can be predicted with relative precision using established theoretical frameworks, shear-related issues lack a universally accepted conceptual model [1]. Ductile failure provides a clear warning signal, such as plastic deformation, while brittle failure occurs suddenly, offering minimal warnings. This distinction is crucial because, under shear forces, concrete exhibits rapid crack development without the gradual yielding seen in flexural failures. With the growing demands on bridge structures due to increasing traffic loads, particularly from heavy goods vehicles, the need for advanced monitoring and assessment techniques are expected to intensify in the coming years [3]. Current methods for shear monitoring rely mostly on visual inspections, which are labor-intensive, subjective [4], and not effective when surface damages are not present in the structure.

As shear load-bearing behavior remains a challenging aspect of structural evaluation, innovative monitoring technologies such as distributed fiber optic sensors (DFOS) offer promising solutions to ensure the safety, durability, and sustainability of critical infrastructure. To improve the efficiency and precision of crack detection, integrating continuous strain monitoring systems like DFOS can provide real-time, comprehensive data on damage states [4]. DFOS can accurately measure small strain changes during the linear elastic state, an advantage that surpasses traditional visual inspections in terms of objectivity, repeatability, and sensitivity. Although the application of fiber optic sensing in construction is relatively recent, the technology is rapidly evolving and has shown potential in various infrastructure applications [5]–[8]. Low-cost optical fibers that serve as sensors can be retrofitted onto existing structures or embedded into new constructions, providing a convenient approach for distributed structural health monitoring.

Inspired by the shear monitoring concepts [2], [9]–[13], this paper presents an application of a DFOS grid for crack monitoring in a prestressed concrete girder. The aim is to further investigate the potential and to assess the effectiveness of surface-bonded DFOS for microcrack detection, formation, and the sensor placement for short-term monitoring. A two-dimensional DFOS grid was designed and applied to the surface of a prestressed concrete bridge girder, which was

DOI: 10.3217/978-3-99161-057-1-029

subsequently tested under load. Following a brief state-of-the-art review in Chapter 2, the experimental setup and corresponding results are presented.

2 SHEAR BEHAVIOR AND DIAGNOSTICS

2.1 Critical shear behavior

Concrete bridges, especially those older than 30 years old, were designed under shear-reinforcement rules now known to be insufficient for modern traffic loads, and routinely exhibit calculated shear deficits, which raise significant concerns about their long-term structural performance [14]. The shear failure is governed by diagonal cracking: when inclined tensile stresses (highest near supports) exceed the concrete's tensile strength, a rapid chain of web-shear cracks propagates toward loading areas and supports, often with little warning [15], [16]. When a beam is subjected solely to pure bending, tensile stresses that exceed the concrete's tensile strength will cause vertical cracks to form and extend up to the neutral axis. However, when shear forces are present, they cause the flexural cracks to rotate, resulting in flexural-shear cracks, which are typical in slender reinforced concrete girders subjected to shear. In flanged girders, deep girders, and prestressed ones, the dominant shear failure mode is web-shear cracking. Cracks initiate at the beam's centroid where the principal elastic tensile stress exceeds the concrete strength, and then extend toward both the loading area and the supports [16].

Concrete shear resistance arises from aggregate interlock, dowel action of longitudinal bars, and, in deep members, arch action. Geometry (shear-span/depth ratio) and reinforcement ratios critically govern which mechanism dominates [15]. Moreover, large members display a pronounced size effect, failing more abruptly. Analytical frameworks, such as strut-and-tie models, compression field theory, and critical shear-crack theory, seek to capture these phenomena, but each has limitations when applied to prestressed girders, where axial compression and anchorage stresses further complicate shear behavior [1], [17]. This sudden and complicated failure mode underscores the need for continuous monitoring systems, such as DFOS grids, to detect microcrack initiation and propagation before diagonal crack development.

2.2 Need for shear monitoring

Following the bridge recalculation and assessment guideline (May 2011), Fischer et al. [18] performed the statical recalculation of 115 bridges' superstructure that required shear reinforcement, and 57% of them exhibited low shear capacity. Notably, it is the case that some of these structures do not display visible shear cracks. This highlights the need to implement a monitoring system that measures the development and long-term performance of these structures, to accurately estimate the remaining service life and ensure the safety of the infrastructure [2], [4], [16]. Critical shear behavior is primarily marked by the development of diagonal cracks, which present challenges in early detection. These cracks, which form at inclined angles relative to the beam's axis and do not align with the reinforcement, are inherently more unpredictable than flexural cracks. The heterogenous nature of concrete, diagonal cracks' orientation, and variable crack width introduce significant uncertainties in early crack detection and crack propagation [19], [20]. Consequently, effective shear measurement systems are essential for reliable structural analysis and monitoring of shear failures [15].

Currently, shear monitoring predominantly relies on visual inspection of the concrete surfaces [4]. While this approach can reveal surface-level damages, it is labor-intensive and susceptible to human error, potentially leading to missed early signs of deterioration [4].

Developing a robust measurement concept for shear monitoring in real-world bridge applications is a challenging problem. While controlled laboratory conditions allow for predetermined critical sections and failure locations, practical implementations face challenges such as limited sensor measurement range, harsh environmental conditions, and economic constraints. These factors increase the risk of missing critical zones during monitoring. To overcome these challenges, there is a clear need for an innovative, autonomous, and robust measurement system, potentially leveraging advanced techniques like DFOS and digital image correlation (DIC), to accurately reflect the evolving structural state and enhance long-term infrastructure safety [4].

2.3 Distributed fiber optic sensing (DFOS)

Fiber optic measurement has evolved remarkably over the recent decades. Initially developed for telecommunications [21], its adoption in structural health monitoring (SHM) within the construction industry has surged, particularly for concrete structures [22]. They offer a unique advantage by providing continuous, high-resolution strain data over entire structural elements, an attribute that is very valuable for monitoring complex damage patterns associated with shear failure. Because of the relatively recent application of fiber optics in concrete construction, the field is developing dynamically in both research and industry [23].

Unlike conventional sensors, which provide data at discrete points, DFOS capture the full strain distribution along their length with high resolution, enabling the early detection of microcracks and the tracking of crack initiation, propagation, and width changes [24]. By continuously mapping strain across large areas, DFOS can reveal subtle changes in crack patterns that might otherwise remain undetected.

DFOS can be integrated into new structures during construction or retrofitted onto existing bridges. When embedded, they offer immediate insights into load-bearing behavior, prestressing levels, and deformation characteristics [25], [26]. Whether surface-bonded in retrofit scenarios or embedded during construction, DFOS provide real-time strain data to validate structural models and support continuous, long-term performance monitoring. In retrofit applications, bonding DFOS to the concrete surface also enables the direct identification of strain hotspots for targeted inspections. Advanced techniques even allow the derivation of 2D strain images from 1D strain curves, which can be used to get a direct understanding of the situation and stress/strain-state [27]. Given that diagonal cracking is a defining feature of shear failure, a complex and unpredictable 2D phenomenon, employing DFOS is a highly promising approach for SHM.

Because of their ability to monitor the crack pattern over large areas, several research groups [2], [9]–[13] have investigated the possibility of utilizing DFOS for creating a shear monitor concept. DFOS are arranged in a mesh-like manner and installed on the concrete surface to compute 2D strain

DOI: 10.3217/978-3-99161-057-1-029

measurement in the critical shear force zone (as shown in Figure 1). A key advantage of DFOS over other measurement techniques, like DIC, is that they do not require a direct line of sight to the shear-affected area, allowing measurements to be carried out regardless of lighting conditions. By contrast, DIC's noise floor and measurement accuracy are highly sensitive to both the spatial resolution of the images and the size of the measurement field.

Figure 1. 2D sensor arrangement for shear monitoring

The skew angle of the cracks must be taken into account to evaluate the crack widths, since the traditional integration approach that is effective for bending cracks perpendicular to the sensor fails for skewed cracks. In [4], [28], the fundamental process of DFOS-based shear force measurement is explained. A method that incorporates the skew angle into the crack width calculation has been proposed and experimentally validated in [28]. The suitability of DFOS to be used for monitoring shear forces has been confirmed by both laboratory and practical applications. In existing structures, DFOS sensors are typically bonded to the concrete, as demonstrated by Rodriguez et al. [12], [27]. Additionally, Poldon et al. [10] successfully installed DFOS on both longitudinal and transverse reinforcement to track the development of shear and flexural cracks in reinforced concrete beams, a method further validated by practical case studies [9], [13].

Although the initial results are promising, they also highlight the need for further testing and research to rigorously validate the DFOS grid concept's reliability, not only in monitoring shear-induced cracking, but also for tracking the development and precise localization of general bending cracks, to fully determine its practical applicability in real bridge monitoring.

3 TEST AND MEASUREMENT CONCEPT

3.1 Test specimen and test setup

For this experiment, a prestressed concrete girder from a decommissioned road bridge near Ljubljana, Slovenia, was selected for its representative characteristics and historical modifications. Spanning the Kamniška Bistrica River, the bridge measures 52.60 m in length and 8.2 m in width, with five spans ranging from 9 m to 13 m supported by thin wall intermediate supports (Figure 2). Notably, the bridge underwent widening in 1989 to accommodate pedestrians and cyclists by adding prefabricated prestressed reinforced concrete T-girders and an interconnected reinforced concrete slab. The girders and deck were designed with concrete grades MB40 and MB30, which correspond to Eurocode classes C30/37 and C20/25, respectively, in accordance with EN 206-1 and EN 1992-1-1. Prestressing cables with a strength of 1840/2090 MPa were used, while other types of reinforcements, including smooth and ribbed rebars as well as mesh reinforcement, ranged from 240 MPa to 500 MPa.

Six girders were extracted from the structure for laboratory bending and shear tests (see Figure 2). To investigate the girder's behavior under a damaged state, it was deliberately damaged before testing by cutting one of three prestressing layers comprising of six tendons, thereby providing an opportunity to monitor the resulting changes in structural behavior using the DFOS grid.

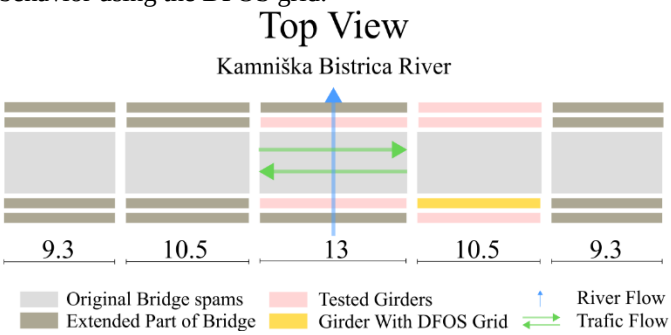

Figure 2. Schematic bridge representation

3.2 Sensor placement and experimental procedure

In the damaged girder, the DFOS grid (as shown in Figure 1) was applied to the web's concrete surface to capture continuous strain data. The DFOS grid consisted of two sensors, with lengths of 12 m and 13 m, respectively. The first sensor (DFOS 1) was arranged in both horizontal and vertical orientations: initially, it was installed horizontally in three parallel layers of 1.6 m segments with a 0.165 m spacing between layers to obtain distinct horizontal strain readings; subsequently, the remaining fiber was configured vertically into 0.33 m segments spaced 0.2 m apart. The second sensor (DFOS 2) was installed diagonally, with each diagonal segment measuring 0.52 m. Additionally, the intersection points of the sensors were aligned as closely as possible, ideally converging at a single point, to enhance data precision and ensure optimal strain transfer. This configuration formed a comprehensive sensing grid capable of capturing crack formation across sensor length, thereby providing a complete strain field of the targeted area. A schematic representation of the sensor layout and test setup is presented in Figure 3.

The fibers employed were single-mode (SM) fibers with a tight buffer made of Hytrel and an overall diameter of 900 µm. Measurements were carried out with an Optical Distributed Sensor Interrogator (ODiSI) 6100 series from LUNA Innovations. This technology leverages the principles of Rayleigh scattering and optical frequency domain reflectometry, providing high-resolution local strain data. The ODiSI was operated in full-optimization mode, delivering a spatial resolution of 0.65 mm and a per-channel measurement rate of 3.13 Hz.

Ensuring optimal bonding to the concrete surface is important for accurate strain measurements. Since the girder was prefabricated, it possessed a smooth finish that required only dust and debris removal. The installation process involved initially fixing the sensor pointwise at predetermined intervals with a fast-curing cyanoacrylate adhesive (CYN), followed by the application of a two-component injection mortar along its entire length. This high-viscosity mortar rapidly hardens and is

DOI: 10.3217/978-3-99161-057-1-029

suitable for bonding sensors on vertical surfaces. At the intersection points, the sensors overlap three times, introducing bending and less reliable results. Figure 3 depicts the DFOS sensor grid configuration and its precise mounting locations on the prestressed concrete girder.

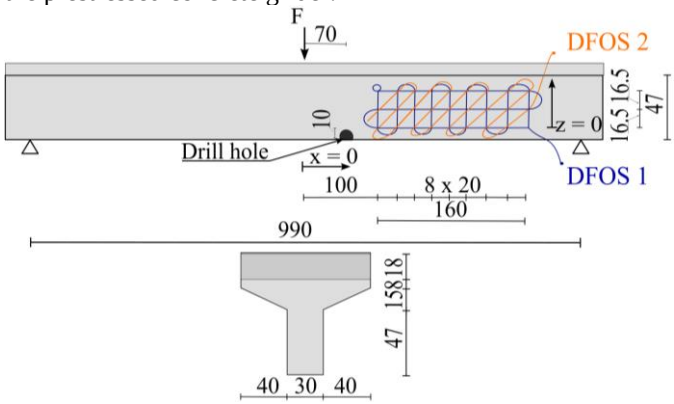

Figure 3. Test setup and cross-section representation (in cm)

Figure 4. Sensor bonding procedure on concrete

After applying the grid, the surface was painted to facilitate DIC measurements. However, the DIC evaluation is beyond the scope of this paper.

Figure 5. DFOS grid covered with DIC speckle pattern

The girder was simply supported on rollers and subjected to three-point bending. The loading test spanned two days and involved cyclic loading and sustained constant load conditions to replicate diverse operational states and observe the crack initiation and propagation phases. In the initial cutting stage, a hole of 10 cm in diameter was drilled to induce damage in the specimen (Figure 6). A full drill-through was performed to cut the bottom layer of tendons, thereby deliberately weakening the girder. This intervention was carried out at a location 70 cm from the loading point, providing a controlled site to monitor the ensuing changes in structural behavior using the DFOS grid.

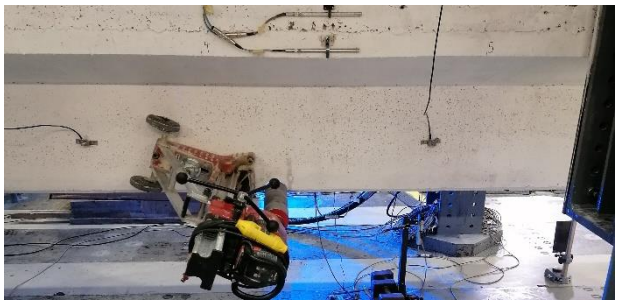

Figure 6. Test initiation with the cutting procedure

4 PRELIMINARY RESULTS

4.1 Load-displacement behavior

Loading was applied under force control at a rate of 1 kN/s (phases P1 to P3), and then under displacement control at a rate of 0.1 mm/s (phases P4 to P6) with a maximum load of 428 kN. Figure 7 shows the load-displacement behavior, where the vertical displacement was measured with a displacement transducer located in the middle of the girder.

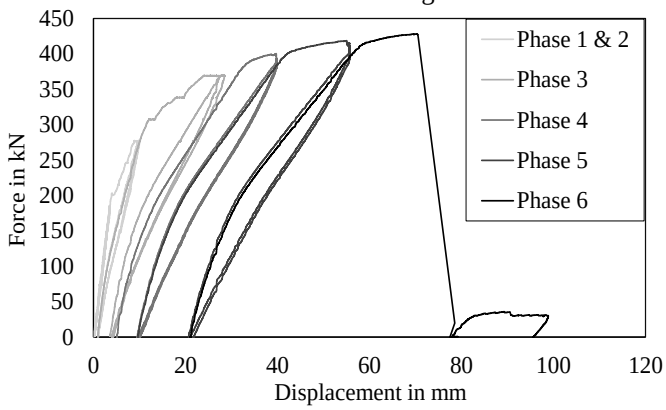

Figure 7. Force-displacement behavior of the girder

The load was gradually increased in six distinct phases, P1–P6, with each phase consisting of two loading–unloading cycles. After the second unloading cycle of each phase, the girder was put to rest for 20 minutes under ambient vibration conditions. Upon completing phase 3 on the first test day, the girder was brought to the phase 3 peak load (369 kN) and maintained at this constant level overnight. On the following day, the load was released (unloading phase) before initiating phase 4, creating three stages between phases 3 and 4: loading, constant force, and unloading.

The graph in Figure 7 illustrates a progressive stiffness reduction and the onset of plastic deformation with increasing load. In the early phases P1-P2, the steep force–displacement slope denotes the girder's high initial stiffness, with visual crack initiation occurring during the first cycle of phase 2 (P2-C1) in the damaged zone. As loading advances into phases P3-P4, the slope diminishes, reflecting stiffness loss from crack propagation and the commencement of permanent deformations. In the final phases P5-P6, approaching the ultimate capacity of 428 kN, the response becomes distinctly nonlinear, marked by successive crack formation and partial yielding of the reinforcement.

In Figure 8 below, the crack patterns on the face of the girder opposite to where the DFOS grid was installed, overlaid with a

DOI: 10.3217/978-3-99161-057-1-029

schematic representation of the sensor layout for comparison, are shown. At the peak load of phase 5, multiple cracks are visible, with crack openings marked directly on the concrete surface during the test. In the region corresponding to the DFOS grid, the first signs of cracking appeared as early as loading phase 3, indicating that the sensor network would have detected these strain concentrations in real time.

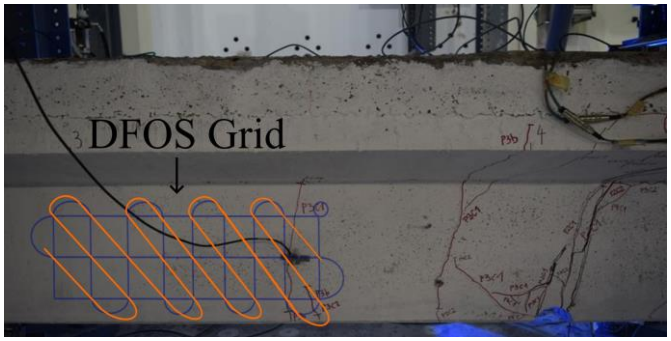

Figure 8. Crack pattern from the other side of the girder at load phase 5 (418 kN)

4.2 Framework and labeling

The data from the DFOS grid was analyzed using the fosanalysis framework (available at https://github.com/TUD-IMB/fosanalysis/) developed at TU Dresden, which enables a streamlined workflow from data parsing and preprocessing to crack detection and crack width estimation [24]. This approach yielded excellent agreement between measured and calculated crack widths across different loading stages, indicating the robustness of both the DFOS system and the analysis framework [29].

The preprocessing procedure within the fosanalysis V0.4 framework involves a series of steps designed to enhance the quality and interpretability of the raw strain data obtained from DFOS. Initially, the so-called Strain Reading Anomalies (SRA) are removed using the Global Threshold Method (GTM), where a strain threshold of 300 µm/m is applied to eliminate extreme or unphysical values. Following this, data recorded during phases of constant load are aggregated over time by computing the median value of several consecutive readings, thereby reducing short-term fluctuations and improving stability. Data dropouts, instances where sensor readings are missing or corrupted, are linearly interpolated. To further enhance the signal quality, a sliding mean filter with a window radius of 2 is applied, which smooths the strain profile by averaging adjacent values. A detailed explanation of each method and its implementation is provided in [30].

Figures 9 and 10 plot the peak strains recorded along the DFOS 1 and DFOS 2 sensors at the maximum load of each phase, confirming that a surface-bonded sensor grid, installed without surface grooving, can reliably capture strain evolution under short-term loading. On the horizontal axis of the graphs in figures 9 and 10, sensor lengths are shown; the vertical axis displays strain with maximum peaks of around 3500 µm/m and 4000 µm/m, respectively. High strain peaks started to appear during load phase 3, corresponding well with crack initiation marked with red in Figure 8. During phase 5 of the loading test, the highest strain peaks were recorded. It should be noted that some of the observed strain peaks are associated with sensor turns, and these locations must be carefully accounted for in the analysis, not to be addressed as crack indicators. The true regions of interest are listed in Table 1 below.

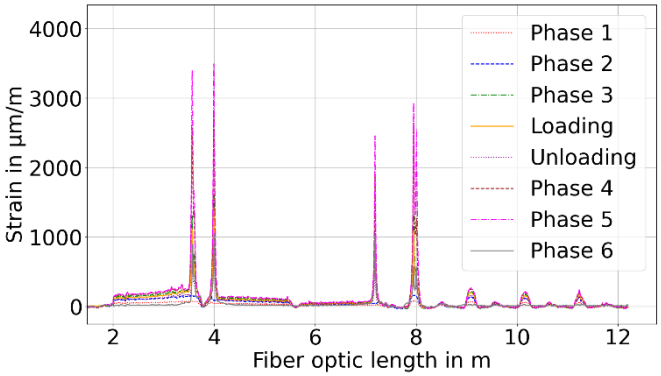

Figure 9. Strain Profile from DFOS 1

An important aspect to be noted is the documentation of the sensor installation, including the exact lengths of sensor segments, starting positions of the grid, and loop configurations. Such detailed records are essential for distinguishing between strain peaks arising from actual structural behavior and those that may result from sensor turns or installation artifacts.

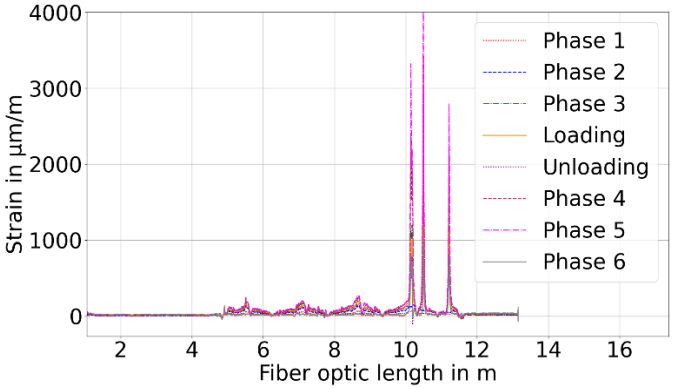

Figure 10. Strain profile from DFOS 2

By defining segments and specifying the length range of strain readings, the analysis was divided into horizontal and vertical components for DFOS 1 and diagonal components for DFOS 2. This allowed for accurate localization of areas of interest and targeted data cuts, thereby improving the reliability of crack detection and width estimation at different loading phases.

4.3 Segment cuts and crack detection

Table 1 summarizes the segment crops analyzed for strain peak identification. For DFOS 1, three horizontal layers: bottom, middle, and top, were identified in the region surrounding the primary flexural crack at approximately 3.6 m, 4.0 m, and 7.0 m along the fiber, as confirmed by the crack pattern in Figure 8. Two vertical segments (segments 1 and 2) in DFOS 1 were also selected, with a prominent strain peak observed near the 8.0 m mark. Strain readings were measured in the sensor length between 5 to 12 m for DFOS 2. Within this range, inclined segments labeled 7, 8, and 9 exhibited significant strain peaks and were therefore selected for detailed analysis.

DOI: 10.3217/978-3-99161-057-1-029

Table 1. Cropped region summary

Cropped Region	Sensor Length Range (m)
Bottom Crop (DFOS 1)	1.98-3.76
Middle Crop (DFOS 1)	3.86-5.56
Top Crop (DFOS 1)	5.64-7.28
Vertical 1 (DFOS 1)	7.42-7.77
Vertical 2 (DFOS 1)	7.79-8.145
Inclined 7 (DFOS 2)	9.335-9.855
Inclined 8 (DFOS 2)	10.075-10.595
Inclined 9 (DFOS 2)	10.865-11.3

By using DFOS, early-stage strain peaks can be identified, allowing for the detection and measurement of potential crack widths. As shown in Figure 11, during phase 3 of the test, the horizontal parts of the sensor exhibit strain peaks ranging from 80 µm/m (top segment) to 300 µm/m (bottom, vertical and inclined segment). These readings indicate a potential onset of crack formation, providing valuable insights into the early development of damage in the beam and allowing monitoring of the structures in the early stages. In the horizontal and inclined segment plots (a, c), the vertical axis denotes strain, while the horizontal axis indicates the sensors' relative positions. For the vertical segment plot (b), the axes are swapped.

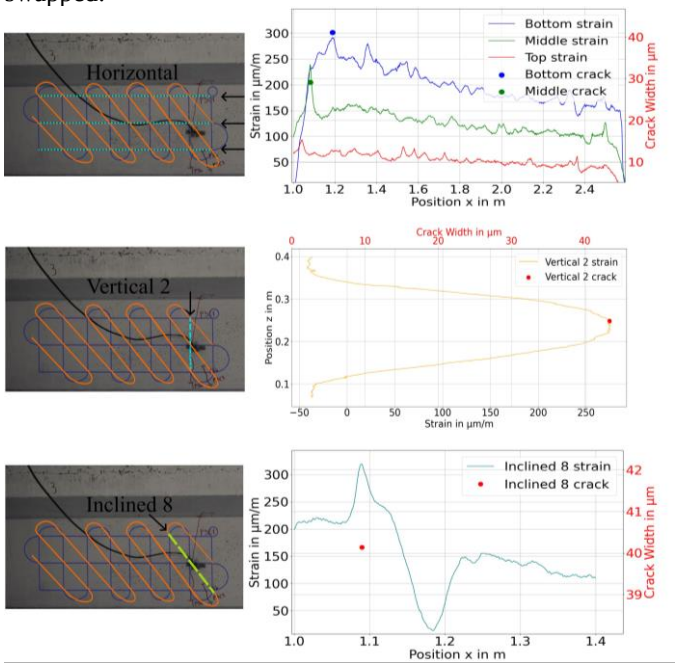

Figure 11. Early-stage DFOS strain profiles indicating incipient crack formation (a) Horizontal, (b) Vertical, and (c) Inclined segments

Building on these early observations, the evolution of strain profiles in three directions of the grid is analyzed. In Figure 12, the measured strain profiles of the horizontal segments of DFOS 1 (top, middle, and bottom) reveal a clear bending response. The readings are shown in temporal order, starting with loading up to phase 3, unloading part, and then loading in phase 5. The top segment exhibits strain peaks up to 2500 µm/m, while the middle and bottom segments reached peaks up to 3500 µm/m. Notably, prominent strain peaks at the bottom correspond to the initial bending crack detected in Figure 11 (a), which becomes more pronounced as load levels increase and the crack propagates further into the beam cross-section.

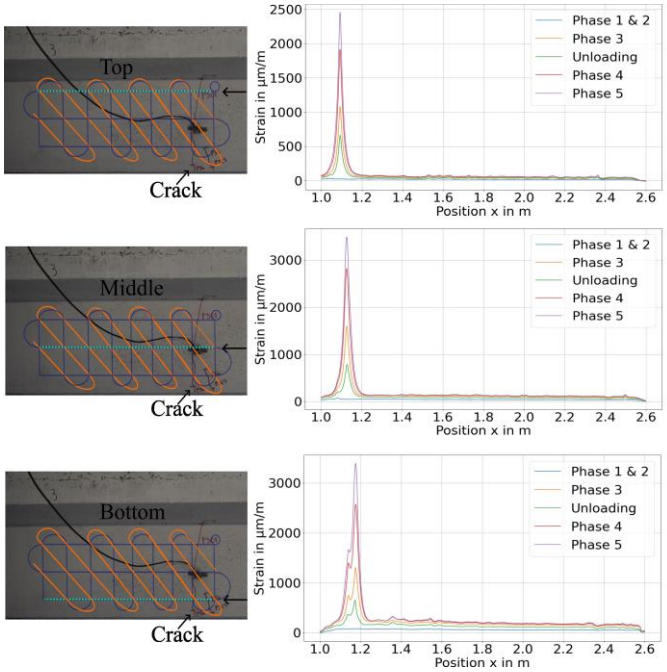

Figure 12 Horizontal strain profiles (a) Top, (b) Middle, and (c) Bottom for DFOS 1

Progressing from the top to the bottom segment, an increase in strain magnitudes can be observed, indicating the development of a crack near the left side of the sensor grid, in the region between 1.2 m to 1.4 m from the origin (check Figure 3). These peaks remain even after the unloading phase, marking a potential crack opening, which is also identified in the corresponding image of the girder. Even after the unloading phase, notable strain remains, indicating the presence of residual crack widths and partial permanent deformation in the beam. These peaks could also be detected by the diagonal and vertical segments, as will be seen in Figures 13 and 14 below.

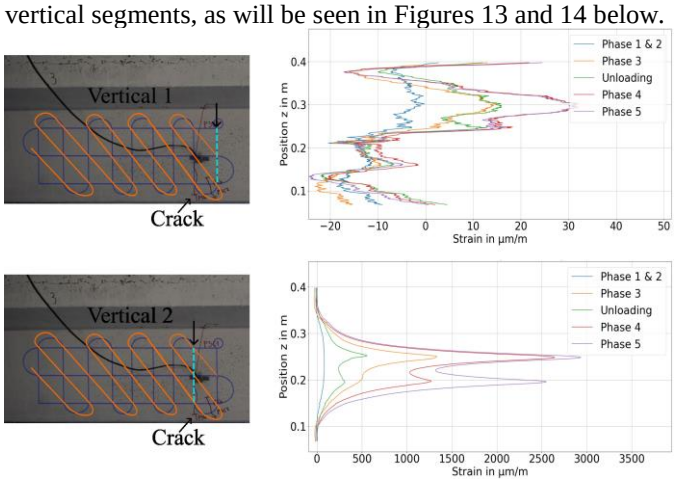

Figure 13. Vertical strain profiles (Vertical 1 and 2) from DFOS 1

The measured vertical strain profiles (Figure 13), under the same load steps, correspond well with the expected structural response of the beam. The vertical axis represents the sensor

DOI: 10.3217/978-3-99161-057-1-029

location in the z direction (check Figure 3), while the horizontal axis shows strain in µm/m. Vertical segment 1, located along the left side of the beam, exhibits strain variations indicative of localized stress redistribution. In these regions, negative strains reflect compression, while positive strains indicate localized tensile effects. The strain readings in this segment, although only in a few µm/m, can suggest an interaction between bending and shear forces, likely influenced by crack propagation near the sensor grid.

The vertical segment 1 remains within ±30 µm/m, indicating a low-stress or compression zone near the neutral axis. As the load increases, the strain peaks in segment 2 become more noticeable (up to 2500 µm/m) in the region between 0.2 m to 0.3 m in z direction. This peak is also an indicator that a crack has been formed in this region, similar to the horizontal readings from the DFOS 1, which detected crack initiation from an early stage (Figure 11) and propagation in both directions.

Figure 14 presents the strain profiles measured along three diagonally oriented segments (labeled inclined 7, 8, and 9, check Table 1) under the same load steps as for DFOS 1. The horizontal axis denotes the relative sensor position in the x direction (origin at x = 0), and the vertical axis shows strain measurement. In these diagonal segments, located within a region of potential crack formation, distinct differences in strain behavior were observed.

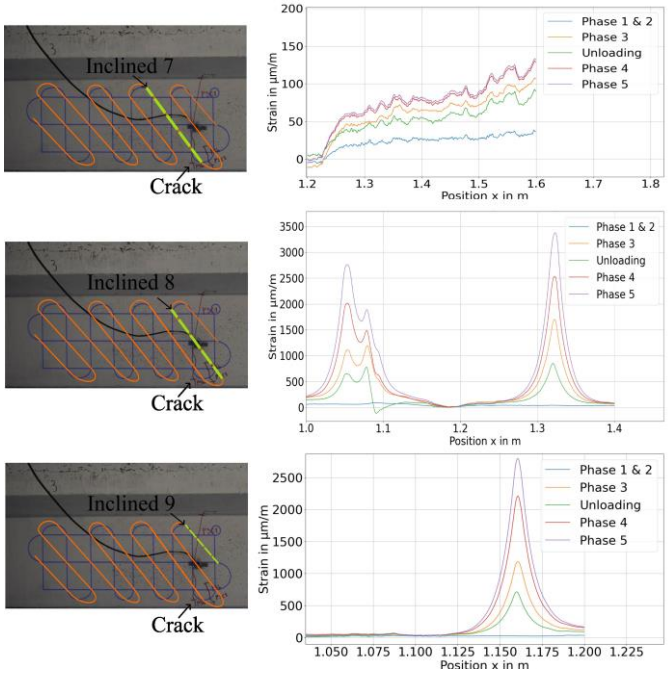

Figure 14 Strain profiles in diagonal segments 7-9 from DFOS 2

Segment 7 displayed a steady increase in strain with loading but showed no pronounced peaks (up to 120 µm/m), suggesting that no major crack crossed this particular sensor path. In contrast, segments 8 and 9 exhibited prominent strain peaks under higher loads (between 2500 µm/m to 3500 µm/m), especially segment 8, where two distinct peaks of 2700 µm/m and 3400 µm/m were observed. This suggests a concentration of cracking or stress in a relatively confined zone. The difference in peak heights for various load steps also demonstrates how the crack opening widens under load and partially closes upon unloading.

The prominent peaks in each plot correspond to localized cracking, which was successfully detected and quantified by the DFOS grid. Furthermore, strain readings in vertical (vertical 2) and inclined sections (inclined 8) reveal the presence of two distinct strain peaks, which may be attributable to crack branching phenomena.

Despite initial expectations to capture diagonal cracking, such cracks were not observed within the grid region. However, the DFOS grid effectively captured and localized vertical cracks from early stages, confirming its potential as a robust tool for structural health monitoring (SHM). The experimental results indicate that for short-term measurements, good bonding between the optical fiber and the concrete surface can be achieved without the need to mill a groove. However, for long-term monitoring under varying environmental conditions, DFOS installation in grooves is recommended. Notably, as observed in the research [23], DFOS sensors installed without grooves can capture higher strain peaks.

Overall, the DFOS-based monitoring proved effective in capturing the strain behavior of the prestressed bridge beam. The results validate the early detection of cracks, well before they become visible to the human eye, similarly to previous research [24] and provide a detailed understanding of crack evolution under varying load conditions. The observed strain peaks could be partially validated through experimental visualization, as evidenced by the crack pattern visible on the opposite side of the beam. Early registration of cracks, especially shear cracks, can be critical, as the development of small shear cracks in large critical regions can, with increasing load, precipitate a sudden shear collapse of the entire reinforced concrete structure.

5 CONCLUSION

The experimental investigation demonstrates that the surface-bonded DFOS grid can be reliably installed without grooving and delivers effective short-term monitoring of prestressed concrete girders. Its high spatial resolution enabled the early detection of microcracks and captured the subsequent growth and spatial pattern of vertical cracks. Strategic sensor placement proved essential for localizing damage zones. These promising results lay the groundwork for advanced structural health monitoring of concrete bridges. Future work at the openLAB Research Bridge in Bautzen, Germany [26], will further validate and refine this DFOS-based monitoring concept.

ACKNOWLEDGMENTS

The authors gratefully acknowledge the financial support provided by the German Federal Ministry for Digital and Transport (BMDV) through the research project *ANYTWIN* (Standardizing Monitoring-Based Safety Assessments of Bridges and the Integration into Digital Twins, funding reference: 01F2248B), funded within the mFUND innovation program.

The authors would like to express their gratitude to colleagues from Technische Universität Graz for their assistance during the installation and measurement of the DFOS grid. Special thanks are also due to colleagues at the Slovenian National

DOI: 10.3217/978-3-99161-057-1-029

Building and Civil Engineering Institute (ZAG) for their expertise in conducting the experimental tests and coordinating critical aspects of the research. The authors acknowledge the financial support from the Slovenian Research and Innovation Agency: Research core funding No. P2-0273 and Infrastructure funding I0-0032.

REFERENCES

[1] M. Herbrand, 'Shear strength models for reinforced and prestressed concrete members', RWTH Aachen University, 2017.
[2] H. Becks et al., 'Monitoring the Fatigue-Induced Strain Evolution of Concrete Bridges using Fiber Optic Sensors', *ce papers*, vol. 6, no. 5, pp. 1119–1126, Sep. 2023.
[3] M. Herbrand and J. Hegger, *Assessment of the shear capacity of existing bridges – short term solutions*, 2014.
[4] H. Becks et al., 'Measuring Strain and Crack Evolution in Reinforced Concrete under Monotonic and Fatigue Tension using Fiber Optic Sensors', *Procedia Structural Integrity*, vol. 64, pp. 1279–1286, Jan. 2024.
[5] W. Lienhart et al., 'Distributed Vibration Monitoring of Bridges with Fiber Optic Sensing Systems', in *Experimental Vibration Analysis for Civil Engineering Structures*, Cham, 2023, pp. 662–671.
[6] Ł. Bednarski et al., 'New Distributed Fibre Optic 3DSensor with Thermal Self-Compensation System: Design, Research and Field Proof Application Inside Geotechnical Structure', *Sensors*, vol. 21, no. 15, p. 5089, Jul. 2021.
[7] M. Bertulessi et al., 'Experimental Investigations of Distributed Fiber Optic Sensors for Water Pipeline Monitoring', *Sensors*, vol. 23, no. 13, p. 6205, Jan. 2023.
[8] C. M. Monsberger et al., 'Large-scale distributed fiber optic sensing network for short and long-term integrity monitoring of tunnel linings', *J Civil Struct Health Monit*, vol. 12, no. 6, pp. 1317–1327, Dec. 2022.
[9] S. Gehrlein and O. Fischer, 'Großversuche zur Querkrafttragfähigkeit bestehender Spannbetonbrücken an der Saalebrücke Hammelburg', *Beton- und Stahlbetonbau*, vol. 113, no. 10, pp. 696–704, 2018.
[10] J. J. Poldon et al., 'Distributed Sensing in Large Reinforced Concrete Shear Test'.
[11] O. Fischer et al., 'Quasikontinuierliche faseroptische Dehnungsmessung zur Rissdetektion in Betonkonstruktionen', *Beton- und Stahlbetonbau*, vol. 114, no. 3, pp. 150–159, 2019.
[12] G. Rodriguez et al., 'Shear crack pattern identification in concrete elements via distributed optical fibre grid', *Structure and Infrastructure Engineering*, vol. 15, no. 12, pp. 1630–1648, Dec. 2019.
[13] B. Novák et al., 'Neues Potential im Structural Health Monitoring : Verteilte faseroptische Sensoren für Bestandsbauwerke', in *12. Symposium Experimentelle Untersuchungen von Baukonstruktionen*, 2023.
[14] J. Hegger 'Assessment of the shear and torsion capacity of existing bridges - extented design approaches', Bremen: Fachverlag NW in der Carl Ed. Schünemann KG, 2020.
[15] G. Schacht et al., 'Experimentelle Bewertung der Schubtragsicherheit von Stahlbetonbauteilen', *Beton und Stahlbetonbau*, vol. 111, no. 6, pp. 343–354, Jun. 2016.
[16] P. Valerio, *Realistic shear assessment and novel strengthening of existing concrete bridges*, the University of Bath's research portal, 2009.
[17] T. Hertle, 'On Mechanical Shear-Models in Reinforced and Prestressed Concrete Constructions'. Universit at der Bundeswehr Munchen, Nov. 2023.
[18] O. Fischer et al., *Nachrechnung von Betonbrücken - systematische Datenauswertung nachgerechneter Bauwerke*. Bremen: Fachverlag NW, 2016.
[19] G. Rodríguez et al., 'Shear crack pattern identification in concrete elements via distributed optical fiber grid.'
[20] T. Wu et al., 'Recent Progress of Fiber-Optic Sensors for the Structural Health Monitoring of Civil Infrastructure', *Sensors*, vol. 20, no. 16, p. 4517, Aug. 2020.
[21] L. Stiny, *Passive elektronische Bauelemente, 2019*.
[22] M. F. Bado and J. R. Casas, 'A Review of Recent Distributed Optical Fiber Sensors Applications for Civil Engineering Structural Health Monitoring', *Sensors*, vol. 21, no. 5, p. 1818, Jan. 2021.
[23] M. Herbers et al., 'Crack monitoring on concrete structures: Comparison of various distributed fiber optic sensors with digital image correlation method', *Structural Concrete*, Jun. 2023.
[24] B. Richter et al., 'Towards an Automated Crack Monitoring using Distributed Fiber Optic Sensors', *ce papers*, vol. 6, no. 5, pp. 635–643, Sep. 2023.
[25] B. Richter et al., *Monitoring of a prestressed bridge girder with integrated distributed fiber optic sensors*, vol. 64. 2024, p. 1215.
[26] M. Herbers et al., 'openLAB – Eine Forschungsbrücke zur Entwicklung eines digitalen Brückenzwillings', *Beton- und Stahlbetonbau*, vol. 119, no. 3, pp. 169–180, 2024.
[27] G. Rodriguez et al., 'Shear crack width assessment in concrete structures by 2D distributed optical fiber', *Engineering Structures*, vol. 195, pp. 508–523, Sep.
[28] X. Lu and S. Zhang, 'Investigation of Mixed-Mode Crack Quantification with Distributed Fiber Optic Sensors', *e-Journal of Nondestructive Testing*, vol. 29, Jul. 2024.
[29] M. Herbers et al., 'Rayleigh-based crack monitoring with distributed fiber optic sensors: experimental study on the interaction of spatial resolution and sensor type', *J Civil Struct Health Monit*, Dec. 2024.
[30] B. Richter et al., 'Advances in Data Pre-Processing Methods for Distributed Fiber Optic Strain Sensing', Nov.2024.